

NO-A143 720

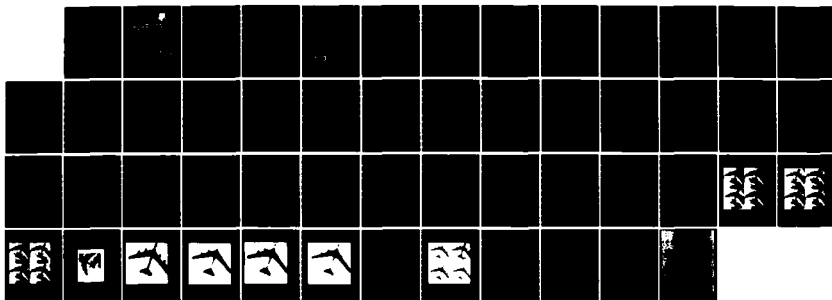
AN EVALUATION OF IMAGE RESTORATION FILTERING FOR  
MACHINE CLASSIFICATION APPLICATIONS(U) ROME AIR  
DEVELOPMENT CENTER GRIFFISS AFB NY D C LAI ET AL.  
MAR 84 RADC-TR-84-50

1/1

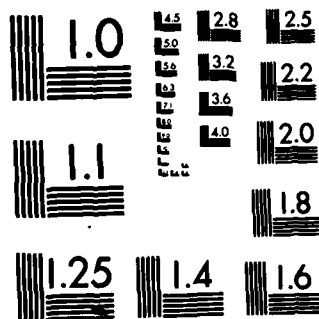
UNCLASSIFIED

F/G 9/2

ML







MICROCOPY RESOLUTION TEST CHART  
NATIONAL BUREAU OF STANDARDS-1963-A

AD-A143 728

RADC-TR-84-50

In-House Report

March 1984

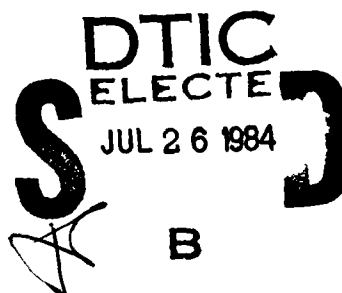


12

# ***AN EVALUATION OF IMAGE RESTORATION FILTERING FOR MACHINE CLASSIFICATION APPLICATIONS***

Dr. David C. Lai, Mr. John Potenza and Mr. Kevin Verfallio

APPROVED FOR PUBLIC RELEASE; DISTRIBUTION UNLIMITED



DTIC FILE COPY

**ROME AIR DEVELOPMENT CENTER  
Air Force Systems Command  
Griffiss Air Force Base, NY 13441**

84 07 26 013

This report has been reviewed by the RADC Public Affairs Office (PA) and is releasable to the National Technical Information Service (NTIS). At NTIS it will be releasable to the general public, including foreign nations.

RADC-TR-84-50 has been reviewed and is approved for publication.

APPROVED: 

GEORGE R. HUGHES  
Assistant Chief, Image Systems Branch  
Intelligence & Reconnaissance Division

APPROVED: 

ALBERT A. JAMBERDINO  
Acting Technical Director  
Intelligence & Reconnaissance Division

FOR THE COMMANDER: 

JOHN A. RITZ  
Acting Chief, Plans Office

If your address has changed or if you wish to be removed from the RADC mailing list, or if the addressee is no longer employed by your organization, please notify RADC (IRRE) Griffiss AFB NY 13441. This will assist us in maintaining a current mailing list.

Do not return copies of this report unless contractual obligations or notices on a specific document requires that it be returned.

UNCLASSIFIED

SECURITY CLASSIFICATION OF THIS PAGE

## REPORT DOCUMENTATION PAGE

1a. REPORT SECURITY CLASSIFICATION UNCLASSIFIED		1b. RESTRICTIVE MARKINGS N/A	
2a. SECURITY CLASSIFICATION AUTHORITY N/A		3. DISTRIBUTION/AVAILABILITY OF REPORT Approved for public release; distribution unlimited.	
2b. DECLASSIFICATION/DOWNGRADING SCHEDULE N/A		5. MONITORING ORGANIZATION REPORT NUMBER(S) RADC-TR-84-50	
4. PERFORMING ORGANIZATION REPORT NUMBER(S) N/A		7a. NAME OF MONITORING ORGANIZATION Rome Air Development Center	
6a. NAME OF PERFORMING ORGANIZATION Rome Air Development Center		6b. OFFICE SYMBOL (If applicable) IRRE	
6c. ADDRESS (City, State and ZIP Code) Griffiss AFB NY 13441		7b. ADDRESS (City, State and ZIP Code) Griffiss AFB NY 13441	
8a. NAME OF FUNDING/SPONSORING ORGANIZATION Rome Air Development Center		8b. OFFICE SYMBOL (If applicable) IRRE	
8c. ADDRESS (City, State and ZIP Code) Griffiss AFB NY 13441		9. PROCUREMENT INSTRUMENT IDENTIFICATION NUMBER N/A	
10. SOURCE OF FUNDING NOS.		11. TITLE (Include Security Classification) AN EVALUATION OF IMAGE RESTORATION FILTERING FOR MACHINE CLASSIFICATION APPLICATIONS	
12. PERSONAL AUTHOR(S) Dr. David C. Lai, Mr. John Potenza, Mr. Kevin Verfaillie*		13a. TYPE OF REPORT In-House	
13b. TIME COVERED FROM Jun 83, to Dec 83		14. DATE OF REPORT (Yr., Mo., Day) March 1984	
15. SUPPLEMENTARY NOTATION *Dr. David Lai and Mr. Kevin Verfaillie are from the University of Vermont		16. PAGE COUNT 56	
17. COSATI CODES		18. SUBJECT TERMS (Continue on reverse if necessary and identify by block number)	
FIELD 09	GROUP 4	SUB. GR. 4	
		Image Processing Restoration Filtering Automatic Pattern Recognition	
19. ABSTRACT (Continue on reverse if necessary and identify by block number) <p>Recently, Rome Air Development Center (RADC) and Defense Mapping Agency (DMA) have procured a software package designed to perform restoration processing on digital imagery. The software package was developed under contractual effort by PAR Technology Inc. and installed on the RADC Image Processing System (IPS) and the DMA Remote Work Processing Facilities which are identically configured and consist of a compliment of PDP 11/34, PDP 11/70, AP120B Array Processor, displays and peripherals.</p> <p>The purpose of this report is to document results of recent experimentation performed at RADC under the Summer Faculty Research Program using the IPS and the Image Restoration and Manipulation Software (IRAMS) package. The report contains the results of a ten (10) week investigation performed by David Lai and Mr. Kevin Verfaillie of the University of Vermont and Mr. John Potenza of RADC (IRRE).</p>			
20. DISTRIBUTION/AVAILABILITY OF ABSTRACT UNCLASSIFIED/UNLIMITED <input checked="" type="checkbox"/> SAME AS RPT. <input type="checkbox"/> DTIC USERS <input type="checkbox"/>		21. ABSTRACT SECURITY CLASSIFICATION UNCLASSIFIED	
22a. NAME OF RESPONSIBLE INDIVIDUAL John Potenza		22b. TELEPHONE NUMBER (Include Area Code) (315) 30-3175	
		22c. OFFICE SYMBOL IRRE	

DD FORM 1473, 83 APR

EDITION OF 1 JAN 73 IS OBSOLETE.

UNCLASSIFIED

SECURITY CLASSIFICATION OF THIS PAGE

# TABLE OF CONTENTS

SECTION		Page
I	OBJECTIVE	1
II	DISCUSSION OF THE RESTORATION PROBLEM	2
III	MATHEMATICAL FORMULATION OF RESTORATION	6
IV	EXPERIMENT CONDITIONS AND CONSTRAINTS	13
V	RESULTS AND DISCUSSION	20
VI	SUMMARY AND CONCLUSIONS	24

**DTIC**  
**ELECTE**  
**S** JUL 26 1984 **D**  
**B**

<b>Accession For</b>	
NTIS GRA&I	<input checked="" type="checkbox"/>
DTIC TAB	<input type="checkbox"/>
Unannounced	<input type="checkbox"/>
Justification	
By _____	
Distribution/	
Availability Codes	
Dist	Avail and/or Special
<b>A-1</b>	



## LIST OF TABLES

TABLE	Page
I    Relative Classification Errors for Metal (Airplane)	27
II   Relative Classification Errors for Soil	28
III   Relative Classification Errors for Shadow	29
IV   Relative Classification Error for all three Classes	30

## LIST OF FIGURES

FIGURE	Page
1    Original Image and Blurred Forms	31
2    Original Image with two levels of Noise Degradation	32
3    Original Image with constant Noise and Various Blurs	33
4    Original Image depicting Supervised Training Regions	34
5    Original Image/Classification via AFES Software	35
6    Classification Results on Degraded/Unrestored Image	36
7    Classification Results on Degraded/Wiener Restored Image	37
8    Classification Results on Degraded/Median Restored Image	38
9    Overall Classification Performance Ranking	39
10   A Test Image Restored via Wiener, Median and Geometric Mean Filtering	40

## ACKNOWLEDGEMENT

The authors wish to thank RADC, Mr. Frederick W. Rahrig for his assistance in using the Image Processing System facility, valuable suggestions in the selection of the classifier used, and assistance in obtaining the photographs used in the figures. In addition they would like to thank Mrs. Janet Piccola for her clerical assistance in preparing and documenting the report.

## BACKGROUND

RADC has supported DMA for a number of years in developing and configuring software and hardware into a test bed Imagery Processing system which has since been installed at DMA Hydrographic & Topographic Center (DMAHTC) and Aero Space Center (DMAAC) and at RADC/IRRE. The system was designed as a user friendly test bed for continued development and evaluation of semi-automatic computer assisted techniques to perform various feature extraction functions. The test bed includes a collection of system and application software modules which support a variety of functions required in the image exploitation process. Application software includes pixel measurement extraction, pixel classification pattern recognition, image enhancements and manipulations, etc. More recently a software subsystem package was developed and installed at each facility providing a capability to perform image restoration operations on digital imagery. This subsystem termed Image Restoration and Manipulation Software (IRAMS) was designed to provide a highly interactive semi-automatic degradation assessment capability and a collection of image restoration filters housed on one computing facility. The IRAMS package represents the most comprehensive single installation of image restoration filters available to date. This software combined with existing and in development image processing and artificial intelligence software offers a unique experimental tool for further research addressing critical image processing issues, algorithm development and digital technology impacting DMA and Air Force evolution to softcopy automatic image exploitation applications.

The purpose of this report is to document results of an effort whereby a number of image restoration filters were experimentally evaluated on the RADC/IPS. The evaluation performed is unique in that restoration performance is evaluated for facilitating machine classification rather than for human interpretation as was the case in known past reported work (10, 11). This route was taken since the image exploitation function is evolving into an automatic operation and required preprocessing functions (i.e. restoration enhancements, etc) should be compatible with and facilitate machine classification and recognition in the long term.

## SECTION I

### OBJECTIVE

1.0 The main objective of this experimentation is to systematically evaluate and compare the performances of different image restoration filters in machine classification so as to ascertain their usefulness in facilitating machine recognition. More specifically, the following items were performed:

(1) Analyze image restoration filters to gain insights that may lead to the development of guideline for practical applications and ideas for designing new filters.

(2) Test and evaluate six restoration filters: Inverse, Wiener, Parametric Wiener, Geometrical Mean, PSE, and Median filter on images of various degrees of degradation based on their performances in machine classification of the scene in the image.

(3) Derive an appropriate performance measure in order to quantify performances of the filters.

(4) Compare these filters under different distortion conditions.

This investigation was not concerned with the interrelationship between restoration filtering, feature extraction and classifying. In other words, the mutual effects between filters, feature extractors, and classifiers were not considered. Moreover, the many image enhancement techniques which undoubtedly, facilitate machine recognition were also not considered.

## SECTION II

### DISCUSSION OF THE RESTORATION PROBLEM

2.0 The image restoration problem is mathematically ill conditioned, hence there is no unique solution. A variety of restoration filters have been proposed 1, 2, 3, 4, 5, 6, 7, notably the Inverse, Weiner, Parametric Wiener, Geometrical Mean, Power Spectrum Equalization (PSE), Pseudo-Inverse, Homomorphic, Kalman, MAP, ML, MEM, Median etc filters. These filters were designed according to different sets of specific mathematical criteria based on various assumptions of the image models. In practice filter performance varies with the type of image, the blur and the noise conditions. It is natural to ask the following question: How well do the various filters enhance human interpretation of the image or facilitate machine recognition? Or which filter is better than the other and under what conditions? Systematic evaluation and assessment of relative performance between filters is badly needed, since it will facilitate judicious selection of filters for use in Air Force automatic target classification and identification systems using high resolution reconnaissance imagery. Furthermore the resultant information will provide insight and a sound basis in designing new filters for similar Air Force image exploitation missions.

This report concentrates on the investigation and evaluation of performance of six image restoration filters; viz, Inverse, Wiener, Parametric Wiener ( $\alpha = \frac{1}{4}$ ), Geometrical Mean ( $\gamma = \frac{1}{2}, \alpha = \frac{1}{4}$ ), PSE, and Median filters. The basic model for a permanently recorded or observed image  $g(x, y)$  is usually given as:

$$g(x, y) = S \left\{ H \left[ f(x, y) \right] \right\} + \text{or } x \text{ n } (x, y) \quad (1)$$

where  $s$  is a function representing the image sensor response;  $H$ , an operator representing the image formation process;  $f(x,y)$ , the original undistorted image or original object images;  $n(x,y)$  a random noise (formulated as either an additive or multiplicative) process due to the record medium and/or electronic circuit used in image recording. The goal of image restoration is to retrieve  $f(x,y)$  from  $g(x,y)$ . To be more precise, the restoration problem may be stated as: given the recorded and distorted image  $g(x,y)$ , knowledge about the type of the noise  $n(x,y)$ , possibly some knowledge of the original image  $f(x,y)$ , and some knowledge about the image formation in terms of the point-spread-function (PSF), estimate the original undistorted image or original object intensity distribution  $f(x,y)$ . The model given in Eq. (1) is too general to be useful in designing restoration filters. In practice, assumptions and approximations are made to render the design and implementation of restoration filters to be reasonably manageable. In many instances, the non-linear function or operator is approximated by a linear one; the image formation is approximated by convolution with a space-invariant point-spread function (SIPSF); and the noise is assumed to be additive white Gaussian. It is apparent that the ill conditioned nature of the restoration problem together with the variety of image model, assumptions and approximations, and mathematical criteria for optimization results in the many different restoration filters available. Moreover, it would be impossible to test and evaluate all of the filters. With the desire to encompass a wide range of restoration filters and to keep computation within the support of "IRAMS" (Image Restoration and Manipulation Software) implemented by PAR Corp for RADAC, the above six filters were selected for evaluation.

Since the Air Force and Defense Mapping Agency are emphasizing machine classification and identification and the restoration filters are intended to be used as preprocessor for a pattern recognition system, it seemed more appropriate to evaluate the restoration filters based on how well they perform for machine classifiers rather than for photointerpreters. Previous image restoration work was aimed at producing "nice looking" pictures to please human observers.<sup>9</sup> However, a lack of knowledge about the psychophysical processes of human vision and a universal criterion for "beauty" hindered efforts in a systematic evaluation and comparison of restoration filters. Cannon, et al<sup>10</sup> did work on the evaluation and comparison of restoration filters based on a mathematical criterion and the judgment of a panel of photointerpreters. They compared three filters, viz, Wiener, PSE, and MAP. They concluded that based on the subjective quality of photointerpreters, all filters perform equally well on Gaussian blurred images regardless of signal-to-noise ratio (SNR) level, blur severity, or image type; however, MAP filter seems to work best on defocused image in high signal-to-noise environment. Based on the particular mathematical criterion (minimum mean square error), the Wiener filter, as expected performed best. Another closely related work<sup>11</sup> aimed at evaluating the effect of degradation of images on photo interpretability and subjective quality without any restoration performed on the images. The criteria which was used in measuring the degradation effect on human observers are:

(a) Performance by trained photo-interpreters (PI's) in the extraction of a set of essential elements of information from degraded photos, and

(b) Subjective quality as scored by the PI's based on the 10-point NATO standardized scale.

Their conclusion was, indeed, that the interpretability has been re proportion to the degree of degradation by both blur and noise; howe noise had less effect in reducing interpretability. Somehow the PI's through noise but not blur. The subjective quality as measured by Scale was worsened in either case when noise was increased but decreased or when noise was decreased but blur was increased. For i PI's, the correlation between subjective quality and interpretability however, for PI's as a group, the mean correlation was high. To knowledge of the authors, there has been no work reported for evaluat restoration filters for machine recognition. However, the effects ( filtering on machine analysis of images, for edge detection, shape anal texture analysis were reported.<sup>12</sup>

SECTION III  
MATHEMATICAL FORMULATION OF RESTORATION

3.0 The image model given in Eq. (1) provides an accurate characterization of image formation but it is too general to be useful for filter design. For most linear filters, the sensor function  $s$  is approximated by a linear function; the image or blur operator  $H$  is assumed to be linear and represented by spatial-invariant point-spread function; and the noise is assumed to be additive. Based on these assumptions the observed image  $g(x,y)$  becomes:

$$g(x,y) = h(x,y) * f(x,y) + n(x,y) \quad (2)$$

where  $*$  signifies two-dimensional convolution and  $h(x,y)$ , the PSF. Six filters were chosen for testing and evaluation as mentioned previously. The first five, viz., Inverse, Wiener, Parametric Wiener, Geometrical Mean, and PSE filters, represent essentially the entire range of linear filters. They were derived based on the linear model given in Eq. (2). Wiener filtering is perhaps the most common restoration method used. Parametric Wiener filtering seems to give visibly good results.<sup>13</sup> Geometrical mean filtering allows the inverse filter to boost the high-frequency components in a controlled fashion.<sup>14</sup> PSE filtering seems to give a pleasing clear picture.<sup>15</sup> The sixth, median filter, is a nonlinear filter which is useful for noise reduction and edge preservation.<sup>8</sup> Thus, the filters chosen for evaluation represent a wide range of available filters. Derivation of these filters can be found in References (1) and (2) and will not be repeated here. A brief mathematical analysis of these filters is given below:

3.1 Inverse filter - Based on the model given in Eq. (2) and the criterion of minimizing the norm (i.e., power) of the noise, the inverse filter expressed as

transfer function is derived as:

$$H_I(\omega_x, \omega_y) = \frac{1}{H(\omega_x, \omega_y)} \quad (3)$$

where  $H(\omega_x, \omega_y)$  is the optical transfer function (OTF); i.e. the 2-D Fourier transform of the PSF  $h(x, y)$  in Eq. (2). The restored image is then

$$\hat{f}(x, y) = \mathcal{F}^{-1} \left[ \frac{G(\omega_x, \omega_y)}{H(\omega_x, \omega_y)} \right] \quad (4)$$

Using the operator matrix and vector notation, and including additive noise, it is seen that

$$\hat{f} = H^{-1} H f + H^{-1} n = f + H^{-1} n \quad (5)$$

which gives the original image  $f$  plus the transformed noise. In the absence of noise and singularities of the filter, one could restore the distorted image to the original form perfectly. It is seen that the inverse filter concentrates on regaining the original image but disregards (even amplifies) the noise. It is reasonable to expect that the inverse filter will perform well if the noise level is low and there are no singular values of  $H(\omega_x, \omega_y)$  for any  $\omega_x$  and  $\omega_y$ . In general, OTF's exhibit a low frequency "hump" and thus  $H^{-1}(\omega_x, \omega_y)$  tends to boost the high-frequency portion of an image.

**3.2 Wiener filter** - Using the linear model in Eq. (2) and minimizing the mean squared error between the original and the restored image one obtains the Wiener filter.

$$H_w(\omega_x, \omega_y) = \frac{H^*(\omega_x, \omega_y)}{|H(\omega_x, \omega_y)|^2 + [S_n(\omega_x, \omega_y) / S_f(\omega_x, \omega_y)]} \quad (6)$$

where  $H(\omega_x, \omega_y)$  is again the OTF;  $S_n(\omega_x, \omega_y)$ , the noise power spectrum density (PSD); and  $S_f(\omega_x, \omega_y)$ , the PSD of original (or desired) image. In practice, d.c. components (if any) in  $S_n$  and  $S_f$  are subtracted. It is obvious that Wiener filtering reduces to inverse filtering in the absence of noise. For this reason, the noise-to-signal ratio term  $[S_n/S_f]$  in the expression of Wiener

filter may be viewed as a modification function that smoothes the inverse filter and even eases the problem created by the singularities of OTF to provide optimum restoration in the presence of noise. The restored image in the frequency domain is:

$$\hat{F}(\omega_x, \omega_y) = \frac{H^*(\omega_x, \omega_y) F(\omega_x, \omega_y)}{|H(\omega_x, \omega_y)|^2 + \left[ \frac{S_n(\omega_x, \omega_y)}{S_f(\omega_x, \omega_y)} \right]} + \frac{H^*(\omega_x, \omega_y) N(\omega_x, \omega_y)}{|H(\omega_x, \omega_y)|^2 + \left[ \frac{S_n(\omega_x, \omega_y)}{S_f(\omega_x, \omega_y)} \right]} \quad (7)$$

where  $F(\omega_x, \omega_y)$  and  $N(\omega_x, \omega_y)$  are the Fourier transforms of sample functions of the original image process and the noise process, respectively. This shows that the restored image consists of somewhat distorted original and reduced noise. In other words, Wiener filter does not concentrate all its effort in regaining (deblurring) the original image but also operates on the noise as represented by the  $\left[ S_n/S_f \right]$  term in the denominator. Since  $|H|^2$  and  $\left[ S_n/S_f \right]$  in the denominator are equally weighted, the effort of Wiener filter in deblurring the image and reducing the noise is equally distributed. If it is desired that more emphasis be put on deblurring and less emphasis on reducing noise, then the influence of the  $\left[ S_n/S_f \right]$  term in Eq. (7) should be reduced so that the Wiener filter behaves more like inverse filter. This leads to the idea of adjusting the effect of  $\left[ S_n/S_f \right]$  term by multiplying it by a factor  $\gamma$  in Eq. (6) which gives rise to the so-called parametric Wiener filter.

The presence of  $H^*(\omega_x, \omega_y)$  in the numerator of Wiener filter tends to make the filtering biased towards the low frequency end. To combat this low-frequency bias the so called geometrical mean filter was developed and will be discussed later.

3.3 Parametric Wiener Filters - Although Parametric Wiener filter could be derived via the heuristic approach discussed previously, it does not provide a sense of optimality nor insight for obtaining the  $\gamma$  value to multiply to the  $\left[ S_n/S_f \right]$  term. Mathematically, using the model in Eq. (2) and minimizing the effective noise-to-signal ratio of the restored image subject to the constraint

that the residual norm between the observed image and the reblurred restored image equal to the norm of the noise results in

$$H_{PW}(\omega_x, \omega_y) = \frac{H^*(\omega_x, \omega_y)}{|H(\omega_x, \omega_y)|^2 + \gamma [S_\eta(\omega_x, \omega_y) / S_f(\omega_x, \omega_y)]} \quad (8)$$

where, in order to obtain optimum filtering in the constrained least-squares sense, the factor  $\gamma$  must be chosen such that the constraint is satisfied. An algorithm for determining this  $\gamma$  value exists.<sup>13</sup>

It is seen from Eq. (8) that when  $\gamma = 1$ , Parametric Wiener filter becomes Wiener filter and when  $\gamma = 0$ , it becomes inverse filter. Choosing arbitrarily a value ( $\gamma \geq 0$ ) will cause the Wiener filter either to behave more like inverse filter ( $\gamma < 1$ ) or to combat noise more vigorously ( $\gamma > 1$ ). The  $\gamma$  value cannot be arbitrarily assigned to obtain optimum filtering. It must be chosen to satisfy the above mentioned constraint.

**3.4 Geometrical Mean filters** - From the previous discussion, it is understood that inverse filtering regains the original image completely in the absence of noise provided the filter is non-singular. However, in the presence of severe noise and/or filter singularities, the inverse filtering will perform badly; it not only will amplify noise but also accentuate both noise and image signal at the singularities. Wiener filter, on the other hand, will restore the image (not perfectly) as well as reduce noise and it can never be singular in the presence of noise; however, it does tend to favor the low frequency portions of the image and thus loses sharp edges. One thought is to combine inverse filter and parametric Wiener filters in such a way as to parameterize the ratio of their effects on restoration. By judicious choice of the parameters, it is hoped that the low frequency dominance of Wiener filter may be lessened while some singularities of the inverse filter may be avoided. Therefore, Geometrical

mean filters are defined as:

$$\begin{aligned}
 H_{GM}(\omega_x, \omega_y) &= [H_I(\omega_x, \omega_y)]^\alpha [H_{PW}(\omega_x, \omega_y)]^{1-\alpha} \\
 &= \left[ \frac{H^*}{|H|^2} \right]^\alpha \left[ \frac{H^*}{|H|^2 + \gamma [S_n/S_f]} \right]
 \end{aligned}
 \tag{9}$$

For  $\delta=1$ ,  $H_{GM}$  changes from a complete Wiener filter to inverse filter when  $\alpha$  changes continuously from 0 to 1. At the geometric mean ( $\alpha = \frac{1}{2}$ ) with  $\gamma = 1$ , and for symmetrical PSF, i.e.  $H(\omega_x, \omega_y)$  is a real function and  $H_{GM}(\omega_x, \omega_y)$  in Eq. (9) becomes

$$H_{GM}(\omega_x, \omega_y) = \left[ \frac{S_f}{|H|^2 S_f + S_n} \right]^{1/2} = \left[ \frac{S_f(\omega_x, \omega_y)}{S_g(\omega_x, \omega_y)} \right]^{1/2}
 \tag{10}$$

which has the same form as the magnitude of PSE filter.

For the range of  $\delta < 1$  and any  $\alpha$  or  $\alpha \geq \frac{1}{2}$  and any  $\delta$ , the inverse filtering effect dominates. On the other hand, for  $\alpha < \frac{1}{2}$  and  $\delta > 1$ , the Wiener filtering effect dominates the scene. Hunt<sup>14</sup> showed that, for moderate blur and low SNR, the geometrical mean filter with  $\alpha = \frac{1}{2}$  and  $\delta = \frac{1}{2}$  produced good result.

**3.5 PSE (Power Spectrum Equalization) filter** - As stated earlier, the inverse filter restores perfectly in the absence of noise, provided there is no singularity in the blur function; however, in the presence of noise, it attempts also to regain the image information in the noise bands and thus accentuates the noise. One way to remedy this is to limit the gain of the restoration filter

for the low SNR bands of the image spectrum. Based on the image model in Eq. (2) and with the constraint that the PSD of the restored image is equal to that of the original image, the PSE filter was derived as:

$$|H_{PSE}(\omega_x, \omega_y)| = \left[ \frac{S_f(\omega_x, \omega_y)}{S_g(\omega_x, \omega_y)} \right] \quad (11)$$

and the phase is set equal to the negative of the phase of the blur spectrum. 15 It is seen that the design of this filter does not require knowledge about the noise (spectrum).

The PSE filter can also be obtained by setting  $\alpha = \frac{1}{2}$  and  $\gamma = 1$  in the design of geometrical mean filters. Thus PSE filtering has the combined effect of inverse filtering and Wiener filtering in equal strength.

3.6 Median filter - Median filters are non-linear filters. This family of filters is not derived on the basis of an image model and a set of mathematical criteria. Median filtering was first suggested by Tukey 16 in 1971 for smoothing time series and noticed its property in preserving large sudden changes of level (edges) in time series. It has later been adapted for use in image processing. Median filtering is performed by moving a window over the pixels of an image and replacing the pixel at the center of the window by a pixel whose value is the median of the original pixel values within the window. It was shown that median filtering preserves sharp edges and is very efficient in smoothing "salt-and-pepper" noise but not very effective in reducing Gaussian noise. 8

The mathematical definition of median filtering is given as follows:

$$M(x_i, y_i) = \overset{\text{MEDIAN}}{W} g(x_i, y_i) \triangleq \text{MEDIAN}[g(x_{i+j}, y_{i+j}); x_{i+j}, y_{i+j} \in W] \quad (12)$$

where  $w$  is the filter window;  $(x_i, y_i)$  denotes a pixel of the image usually the

center pixel of the window and  $(x_n, y_s)$ , a pixel inside the window.  $r$  and  $s$  are varied to cover all the pixels in the window and varying  $i$  and  $j$  to move the window to cover all the pixels in the window and varying  $i$  and  $j$  to move the window to cover another portion of the image. The filter window may take many forms such as line segments, rectangles, squares, circles, crosses, square frames, etc. For border points, the median is usually computed on those points covered by the window (without padding zeros). In general, the number of pixels inside the window is odd; otherwise, the mean of two middle points is taken as the median value. Because of the difficulty involved in the theoretical analysis of median filters, there has been practically no published results. However, efficient median filter algorithms have been developed. 17, 18 Furthermore, many attempts were made to implement median filters in hardware which will perform in real time. 19, 20

A median filter was chosen for evaluation because of its simplicity in design and potential for VLSI implementation. It should be noted that this family of filters was designed mainly for suppression of noise while preserving sharp edges with no attempt or regard to restore a blurred image to its original form. It must be used with caution.

## SECTION IV

### EXPERIMENT CONDITIONS & CONSTRAINTS

4.1 Test Data Base - Because of the time limitation for this project, only one picture was chosen for the image restoration filter evaluation experiment. It is a section of an aerial photo of a test site. The image selected consists of a B-52 on a pedestal, shadows and soil. It was chosen mainly for the reason that the scene can be easily classified by machine. This image is shown in its original undistorted form and blurred forms in Fig 1. The image size is 256 x 256 pixels. In order to create a diverse group of distorted images to allow different filters to work under various conditions, the image was subjected to different degrees of degradation.

Due to, again limitations in time, only one kind of blur was chosen; viz; the blur with a Gaussian PSF. Three levels of Gaussian blurs with standard deviations  $\sigma = 3.5, 4.5$  and  $6.5$  were used. The original and the three blurred images were then subjected to further degradation by additive zero-mean white Gaussian noise. The original is not completely noise free. It has a small amount of noise. Two levels of additive noise corresponding to SNR of 12dB and 5dB were used. Thus, the data base for testing consists of 12 images, which include the original, three images degraded by blur only (shown in Fig 1) two images degraded by additional noise only, (Fig 2) and the others degraded by both blur and noise in combinations of degrees of severity, (Fig 3). The degraded images were restored by six different filters which are described in the previous section. Thus 66 restored images were produced along with the 11 test images and original. The scene of each of the images was classified into three categories, viz., metal (airplane), shadow and soil. The number of pixels classified into each class was then counted via pattern recognition software.

The result of classification performed on the original image was taken as the reference (truth) based on the assumption that the machine can do no better on the degraded images than on the original. It was observed that noise alone had less effect on machine classification. For the ease to compare the effect due to blur the 77 images (11 degraded but unrestored and 66 restored) were divided into three groups according to their noise levels. Each group contains 28 images except the one with the original SNR which has only 21 images. They were then evaluated and compared numerically based on the performance measures which will be described in 4.5.

4.2 Feature selection, classifier and machine recognition - For this investigation two features (average intensity and minimum intensity using a 3 x 3 window) were measured and the condensed nearest neighbor classifier was used as the machine recognition scheme. The features and the classifier were selected by cut-and-try method. No attempt was made to find the best features and the best classifier for use on each of these images; similarly, for the set of training regions used. Undoubtedly, one could better the classification performance on each image by choosing the best features, classifier, and training regions for that particular image, however that would defeat our purpose of evaluating and comparing filters for facilitating machine recognition. For our purpose, the effect on classification due to factors such as training regions, features selected, classifier used, etc must be minimized. Therefore, in the strictest sense, our results pertain only to the specific set of experimental circumstances. However, it is felt that the results obtained may be generalized to other types of images, classifiers, etc. as far as that they are applicable. Fig 4 shows the original reference image along with the training regions selected. Three regions were trained upon for soil in order to obtain a composite measure for that category.

There was also no attempt to select features which were improved or enhanced by particular restoration filters. In other words, the problem of feature selection in relation to the use of restoration filters as preprocessor to machine recognition was not addressed here. The understanding of the interrelation between the preprocessor (filters and enhancements) and the feature extractor is important for any practical application of machine recognition.

4.3 Specific Filter Constraints: For the Parametric Wiener filters used herein,  $\gamma$  was arbitrarily set equal to  $\frac{1}{2}$ . No attempt was made to determine the best  $\gamma$  value. Similarly for the geometric mean filter,  $\alpha$  and  $\gamma$  were chosen arbitrarily to be  $\frac{1}{2}$  and  $\frac{1}{2}$  respectively. Therefore the results reported here are for those special cases of the Parametric Wiener and Geometric Mean filters chosen and caution should be taken in generalization of the results. For the median filter only a 3 x 3 window was used. It is generally known that window size and shape affects filter response however, because of expediency this experiment considered only the 3 x 3 window.

4.4 Software Discussion - Two software packages were employed to carry out the experiment. They are the IRAMS and the AFES (Automatic Feature Extraction System) both of which were developed and installed by PAR Technology Corp for RADC to support R&D and DMA production requirements. Application software provided with the AFES supports pixel measurement extraction, pixel classification, image preprocessing, enhancement, filtering, etc. A complete description of the AFES hardware and software may be found in Technical Report RADC TR 82-200. This software package was used to perform the classification

(para 4.2) on the test imagery. Figures 5, 6, 7 and 8 are representative of the results obtained by using the software to automatically classify test images into the three categories selected (metal, soil and shadow). Fig 5 shows the results obtained on the reference image i.e. original and is used to evaluate performance of restoration for machine classification via the measure derived in para 4.5. Fig 6 shows the classification results on a specifically degraded image, and Figs 7 and 8 give results after that image is restored via two filters with extreme performances. Note the confusion in the lower left corner of the image where a number of soil pixels were misclassified as shadow. Fig 7 (Wiener Filter shows improvement while Fig 8 (Median) is worse than the unrestored/classified image. These results are discussed in more detail in Section V.

The IRAMS software package is integrated into the AFES control and application software. Since IRAMS is structured within AFES, it offers a unique tool for developing and evaluating preprocessing techniques in an automatic pattern recognition feature extraction environment. The IRAMS package contains modules to perform image degradation assessments on real world images, and to design and apply a number of restoration filters to the degraded images. The restoration filters implemented in IRAMS may be grouped as linear and nonlinear. The investigation in this report addressed each of the linear filters. The only non-linear case considered was the median filter implemented as a 3 x 3 window.

4.5 Performance Measure Derivation - In the experiment, after performing classification on the images, pixels classified into each class were counted.

Comparing directly these pixel counts of images restored by various filters is not only cumbersome but also leads to difficulty in ranking the filters. The conventional percentage of correct classification or confusion matrix cannot be used here since it is not feasible to identify each individual pixel as being wrongly or correctly classified; only the number of pixels classified into each class can be counted with little difficulty.

The deviation of the pixel counts per class obtained on the restored images from those counted on the original image gives a measure of the size of the area being wrongly classified. It was thought that this deviation for the particular class would serve as a figure of merit to measure the filter's capability in facilitating the classification of pixels. However, with a little more reflection, the severity of each deviation should be considered since it is more severe to wrongly classify 2 pixels out of 10 pixels than to misclassify 2 pixels out of 100. Therefore, the misclassification index for the  $i$ th class was formulated as:

$$\epsilon_i \triangleq \frac{N_{ai} - N_{ci}}{N_{ci}}$$

(12)

where  $N_{ci}$  = no. of pixels truly belonging to the  $i$ th class.

$N_{ai}$  = no. of pixels actually classified into the  $i$ th class by machine. In our case,  $N_{ci}$  is determined by performing machine classification on the original undegraded image as discussed before. It is noted that  $\epsilon_i$  has a range of

$$-1 \leq \epsilon_i \leq \frac{N_t - N_{ci}}{N_{ci}}$$

where  $N_t$  = total no. of classified pixels in the image. The extreme points in the range indicate that either no pixel is classified into the  $i$ th class or all pixels are classified into it. It is seen then that a negative value signifies that the  $i$ th class is underclassified and a positive value, overclassified. When  $\mathcal{E}_i = 0$ , it indicates the best performance for classifying pixels into the  $i$ th class. However, it does not provide a single-number as an overall performance measure.

Often, it is desirable to have a single-number index to gauge the overall performance in classifying pixels into all classes under consideration. Summing over  $\mathcal{E}_i$  would not do since that allows underclassification and overclassification to cancel each other but both kinds of misclassification are equally harmful. A meaningful overall performance measure is thus defined as

$$\mathcal{E} \triangleq \sum_{i=1}^n \frac{|N_{ai} - N_{ci}|}{N_{ci}} = \sum_{i=1}^n |\mathcal{E}_i| \quad (13)$$

where  $n$  designates the number of classes.

This measure has a theoretical range of

$$0 \leq \mathcal{E} \leq \mathcal{E}_{max}$$

where  $\mathcal{E}_{max}$  is derived under the worst situation when every pixel is classified into the class of the smallest size. Let  $N_{cs}$  be the number of pixels in the smallest class, then

$$\mathcal{E}_{max} = (n-1) + \frac{|N_t - N_{cs}|}{N_{cs}} = (n-2) + \frac{N_t}{N_{cs}} \quad (14)$$

However, in practice, it is more likely that every pixel is swamped into the class of the largest size. In that case, the largest value of  $\mathcal{E}$  that will ever result will be less than the max in Eq. (14). A practical range of values is

$$0 \leq \mathcal{E} \leq (n-2) + \frac{N_t}{N_{cl}}$$

where  $N_{cl}$  is the number of pixels in the largest class. Therefore, in order to apprehend the significance of the values for  $\xi$ , one should always analyze the range of  $\xi$  values that may arise in any particular application. This maximum value may be used to normalize so that the index varies between 0 and 1. The best performance occurs when  $\xi = 0$ . This misclassification index is a good indication of the performance of a filter pertinent to the classification for all  $M$  classes under consideration.

Both types of the misclassification indices were used herein. The class index was employed to evaluate and compare the image restoration for their capability in aiding the classification of pixels into a particular class; the overall measure was used to evaluate and compare the filters on their overall performance in classification for all the classes under consideration.

## SECTION V

### RESULTS & DISCUSSION

The numerical evaluation and comparison of filter performance is based on the misclassification indices (classification errors) described in the previous section. These results are presented in Tables I, II, III and IV. The values of Table I represent the classification errors for the metal (airplane); those of Table II, the errors for the soil; those of Table III, the errors for the shadow; and the values of Table IV, the classification errors for all three classes. Negative values represent underclassification while positive values show overclassification as compared to the original image pixel counts. The consistency and patterns exhibited by these values show the utility of the performance measures derived. The range for the values of each table is listed below:

<u>Table</u>	<u>Range</u>
I	-1 6.0115
II	-1 0.3304
III	-1 8.4608
IV	0 10.4608

The range for the overall misclassification index (Table IV) was computed based on the assumption that every pixel would be classified as shadow when the image is hopelessly degraded. In all cases, a zero value indicates the best performance. Hence, the closer to zero the index value, the better the performance.

The metal is much brighter than soil or shadow and hence easier to classify. However, shadow and soil characteristics are quite similar to begin with and become even more alike after degradation of the image and hence difficult to separate. It is seen from Table I that practically all of the filters facilitated the classification of pixels into metal under any distortion condition. From Tables II and III, it is seen that the performances of filters are not clear cut; some of them facilitated the classification for soil at the expense of shadow and vice versa. For example, Wiener filter improved the classification of pixels into soil and shadow at all noise levels and blur severities of  $\sigma = 4.5$  and  $6.5$ ; however, at  $\text{SNR} = 12$  db and  $\sigma = 6.5$ , it did not improve the soil classification but helped greatly for the shadow classification; on the other hand, at  $\text{SNR} = 5$  db and  $\sigma = 4.5$  it performed well for the soil but badly for the shadow. For the overall performance; i.e., facilitating the classification for all three classes, it is seen from Table IV that at high noise level and severe blur, all filters except the Inverse and Parametric Wiener filters improved overall classification. The behavior of Inverse filter at high noise level and severe blur is expected. The erratic performances of parametric Wiener (PW) and Geometrical Mean (GM) filters proved again the importance of selecting the value  $\gamma$  (for the PW filter) and  $\alpha, \gamma$  values (for the GM filter). The value for  $\gamma$  used for PW filter here does not seem to work well for high level of noise and severe blur condition. The

PSE filter has the worst record (3.5845) among all the filters; this occurred at the original SNR and blur of  $\sigma = 6.5$ . It did improve metal classification but misclassified many soil pixels into the shadow class. As mentioned earlier, the PSE filter limits the gain for the low SNR bands of the image spectrum. After severe blur, at the original SNR, the SNR of the soil band became relatively lower. Hence, many soil pixels became darker and thus were classified as shadow.

The median filter (3 x 3 window) improved the classification of metal for images of high noise and severe blur; for classification of shadows and soil, its performance was mixed. This is in line with its character in preserving contrast while reducing noise. It also showed good overall performance in facilitating classification of pixels into all three classes.

Examining Table IV, filters did not help under noise alone situation even though the filters had filtered out noise. This shows that noise alone has little effect on classification. The filters improved classification in the situations when high noise and severe blur were combined. These results agree somewhat with the results reported in Ref. 11 for human observers as stated in Sec. I of this report. Of course, the results obtained could be due to the characteristics of our particular features (measurements) used in the pattern recognition system. Any generalization of our results must be made with caution.

For ease of comparison, graphs may be constructed from the tables. A typical graph is shown in Fig. 2. The graph represents the group of images at

12 db SNR in Table IV which portrays the overall classification performance. The abscissa of the graph shows the blur severity measured in the standard deviation of the Gaussian blur and the ordinate represents the relative overall classification error within the group. The graph shows that the Wiener filter performed well for all blur severities at 12 dB SNR; the Geometrical Mean Filter ( $\alpha = \frac{1}{2}$ ,  $\gamma = \frac{1}{2}$ ) is best for the blur of  $\sigma = 4.5$  at 12 dB SNR; the PSE and Wiener filters performed at about the same level under the most severe blur; the inverse filter did not work well for the most severe blur at this noise level as expected; the Parametric Wiener filter did not perform well because the value used here was not optimized for this combination of blur and noise; the Median filter did not help at all since there were no sharp boundaries between shadows and soil. The plot shows that at a 12 db SNR level filtering does not improve classification for less severe blur. It is also observed that the line connecting all the UR (unrestored) points in the graph and the line through the middle of the filters intersects at  $\sigma = 3.5$ . Extending, this observation, it seems that at this noise level for a blur less severe than a Gaussian blur of  $\sigma = 3.5$ , one should not use image restoration filter to facilitate machine classification. Other graphs can be constructed for groups of other noise levels. They show similar patterns of behavior except that most of the filters improved classification for less severe blur at high noise level.

## SECTION VI

### SUMMARY AND CONCLUSIONS

The major objective of this work was to evaluate and compare a number of digital restoration filters for facilitating machine classification in support of future automatic feature extraction applications. This objective has not been reported on in the past and represents a novel performance measure for image restoration filtering.

Because of time and funding limitations the study was rather limited. A single test image was selected and subjected to various degrees of blur and noise to form a test data base consisting of 12 images with varying degrees and combinations of degradation. These images were restored via six image restoration filters and subjected to a previously developed image classifier for machine classification. No attempt was made to select optimum features and measures used by the classifier, therefore the results reported herein are constrained to a very specific pattern recognition system based on two feature measurements and a limited test data set. Extreme caution must be exercised in generalizing the results and observations beyond the specifics of the experimentation performed. Nevertheless, the results show that image restoration filtering enhances machine classifications in cases of high noise and moderate to severe blur or a combination of low noise and severe blur.

Although no attempt was made in the study to compare machine classification performance with human interpretability of restored images, a number of observations were made which are consistent with results for human

interpretability reported by others. 10, 11 Notably, blur is a more serious form of degradation than noise alone for both human and machine interpretation.

In order to evaluate performance of restoration filtering for machine classification, a non-subjective performance measure was required. Consequently a performance measure based upon a misclassification of pixel index was derived. This index was refined to obtain a single quantitative number to measure how well a restoration filter performed. This measure was used throughout the experimentation and proved to be a useful means for evaluating individual filter performance and comparing performance between filters. Fig 10 is included to show the results of restoring a specific image by three different filters. If those results were submitted for human interpretation, one can begin to understand the difficulty in defining "best" performance. However, the measure derived in this report provides a useful quantitative performance measure for machine classification.

In conclusion a number of points should be emphasized. The experimentation performed in this study provides results which are useful for consideration in machine classification applications. Because of time and funding constraints, a limited set of experimental conditions were addressed and care should be exercised in generalizing the results obtained. During the performance of the work reported herein, a number of questions arose which should be considered for future research. These questions are paraphrased below in the form of recommendations for future research.

a. What features of a digital image are enhanced through application of restoration filters for machine recognition applications?

b. Determine the set of features which are enhanced by specific filters or sets of filters.

c. How do image restoration filters or enhancement techniques interrelate with feature extractors and classifiers?

The answers to the above questions will provide the technical knowledge required to understand the interrelation between preprocessing (such as restoration filtering), feature extractors and machine classifiers in order to improve upon the performance of an automated feature extraction system as a whole rather than in piecemeal. These issues are essential before image restoration and enhancement can be optimized for machine classification in automated feature extraction applications.

TABLE I - RELATIVE CLASSIFICATION ERRORS FOR METAL (AIRPLANE)

SNR		UR	I	W	PW	GM	PSE	M
Original	2.5	-.0462	-.0414	-.0678	-.0724	-.0625	-.0371	-.0722
	4.5	-.1500	-.1373	-.0623	-.1349	-.0884	-.1399	-.1514
	6.5	-.3528	-.1442	.0593	.1499	-.0645	-.0434	-.1544
12dB	0	.0051	.0063	-.0024	-.0007	.0001	.0077	.0255
	2.5	-.0536	-.0619	-.0422	-.0416	-.0388	-.0413	-.0287
	4.5	-.1470	-.0926	-.1148	-.1446	-.1299	-.1438	-.0750
	6.5	-.2032	.0221	-.2209	-.2237	.0623	-.1970	.1560
5 dB	0	.0136	.0077	.0221	.0111	.0020	.0392	.0506
	2.5	-.0298	-.0065	-.0092	-.0169	-.0102	-.0021	.0225
	4.5	-.1314	-.0635	-.0996	-.0758	-.1936	-.0810	-.0290
	6.5	-.1920	-.2238	-.1467	.0315	-.0980	-.2447	-.1256

Range: -1.000 6.0115

n: standard deviation of Gaussian blur

UR: Unrestored

I: Inverse filtering

W: Wiener filtering

PW: Parametric Wiener filtering ( $\gamma = \frac{1}{2}$ )

GM: Geometrical Mean filtering ( $\alpha = \frac{1}{2}, \gamma = \frac{1}{2}$ )

PSE: Power spectrum equalization filtering

M: Median filtering

Neg. No.: Underclassified

Pos. No.: Overclassified

TABLE II RELATIVE CLASSIFICATION ERRORS FOR SOIL

SNR		UR	I	W	PW	GM	PSE	M
Original	2.5	.0125	.0029	.0150	.0115	.0168	.0112	.0141
	4.5	.0348	.0322	.0162	.0383	-.0121	.0303	.0373
	6.5	-.0345	.0172	.0026	-.1601	-.1312	-.4293	.0357
12dB	0	-.0020	.0182	.0036	.0053	.0105	.0025	.0089
	2.5	.0141	.0212	.0175	.0207	.0209	.0250	.0131
	4.5	.0497	.0330	.0367	.0389	.0245	.0382	.0380
	6.5	-.0233	-.1106	.0642	-.1082	-.0611	.0064	-.2215
5 dB	0	-.0047	-.0039	.0157	.0095	.0081	-.0035	-.0042
	2.5	.0185	.0114	-.0116	-.0086	.0029	.0129	.0127
	4.5	.0300	.0216	.0125	-.0093	.0476	.0043	.0184
	6.5	-.0683	-.0668	-.0207	-.1479	-.0262	-.0475	-.0106

Range: -1.000 - 0.3304

Symbols explained in Table I.

TABLE III RELATIVE CLASSIFICATION ERRORS FOR SHADOWS

SNR		UR	I	W	PW	GM	PSE	M
Original	2.5	-.0263	.0355	-.0150	.0157	-.0350	-.0296	-.0027
	4.5	-.0534	-.0440	-.0315	-.1009	.2055	-.0264	-.0608
	6.5	-.1959	.0709	-.0985	.9365	1.0204	3.1118	-.0456
20dB	0	.0074	.1390	-.0226	-.0367	-.0751	-.0285	.0291
	2.5	-.0283	-.0675	-.0674	-.0915	-.0962	-.1218	-.0541
	4.5	-.1834	-.1098	-.1061	-.0817	.0088	-.0773	.3714
	6.5	.4398	1.4954	-.1583	1.0712	-.3507	.2203	1.3645
5 dB	0	.0153	.0175	-.1411	-.0825	-.0606	-.0281	-.0381
	2.5	-.0910	-.0724	.0947	.8239	-.0066	-.0889	-.1206
	4.5	.3925	-.0680	.2244	.1683	-.0771	.0790	-.0915
	6.5	.7447	.7772	.3450	1.0091	.3185	.6680	.2447

Range: -1.000 — +8.4608

Symbols explained in Table I.

TABLE IV RELATIVE CLASSIFICATION ERRORS for ALL THREE CLASSES

SNR		UR	I	W	PW	GM	PSE	M
Original	2.5	.0850	.0798	.0977	.0996	.1144	.0779	.0889
	4.5	.2382	.2135	.1100	.2741	.3060	.1966	.2495
	6.5	.5832	.2323	.1604	1.2466	1.2162	3.5845	.2358
12 dB	0	.0145	.1641	.0286	.0427	.0857	.0387	.0635
	2.5	.0960	.1507	.1270	.1538	.1559	.1881	.0958
	4.5	.3801	.2355	.2577	.2652	.1553	.2593	.4844
	6.5	.6663	.8891	.4435	1.4031	.4741	.4237	1.7420
5 dB	0	.0337	.0292	.1789	.1031	.0708	.0708	.0929
	2.5	.1393	.0903	.1155	.1093	.0197	.1040	.1558
	4.5	.5539	.1532	.3366	.2533	.3183	.1643	.1388
	6.5	1.0049	1.0678	.5123	1.1885	.4427	.9602	.3809

Range: 0 - +10.4608

Symbols explained in Table I.

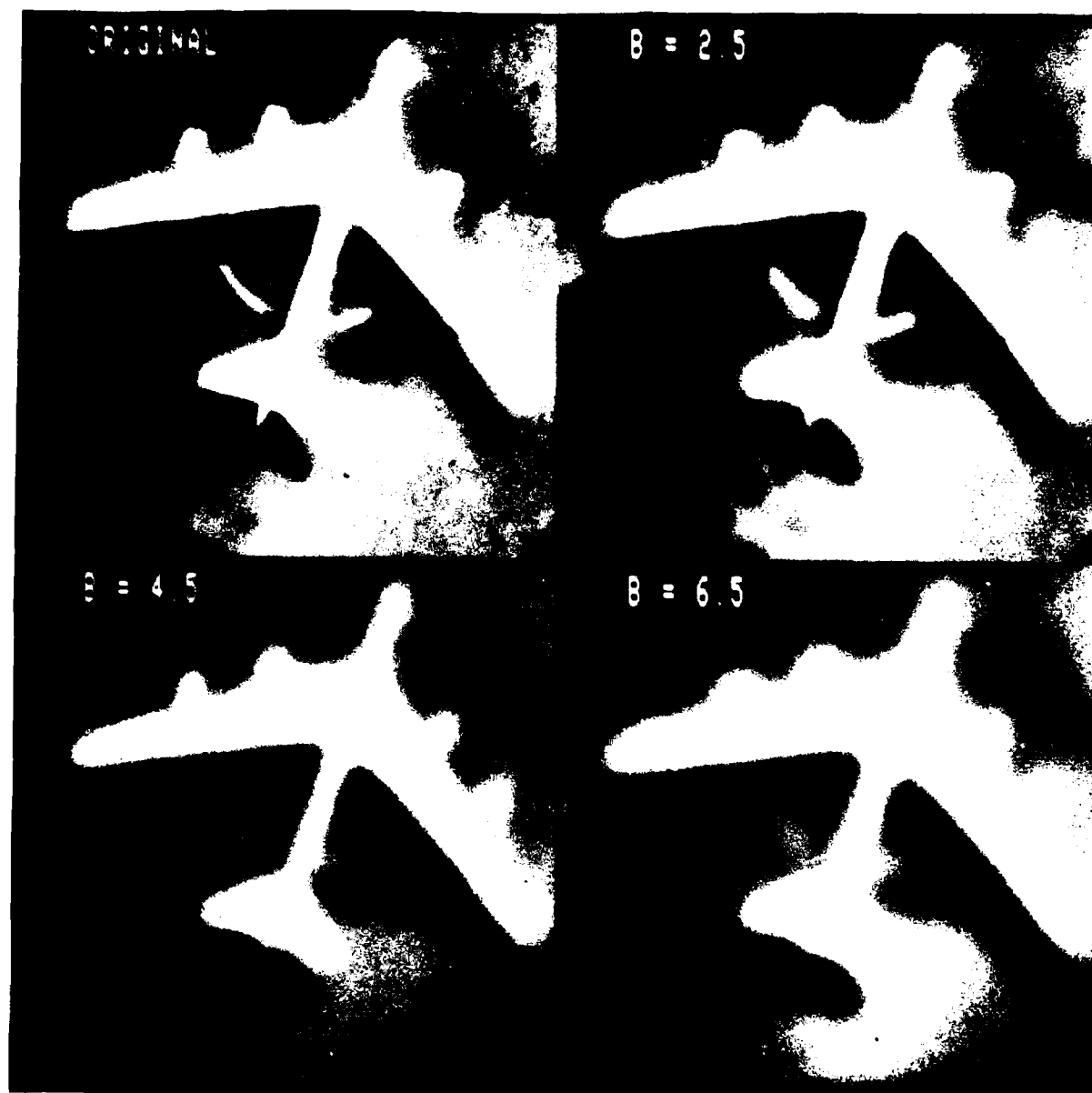


Figure 1 Original Image and Blurred Forms

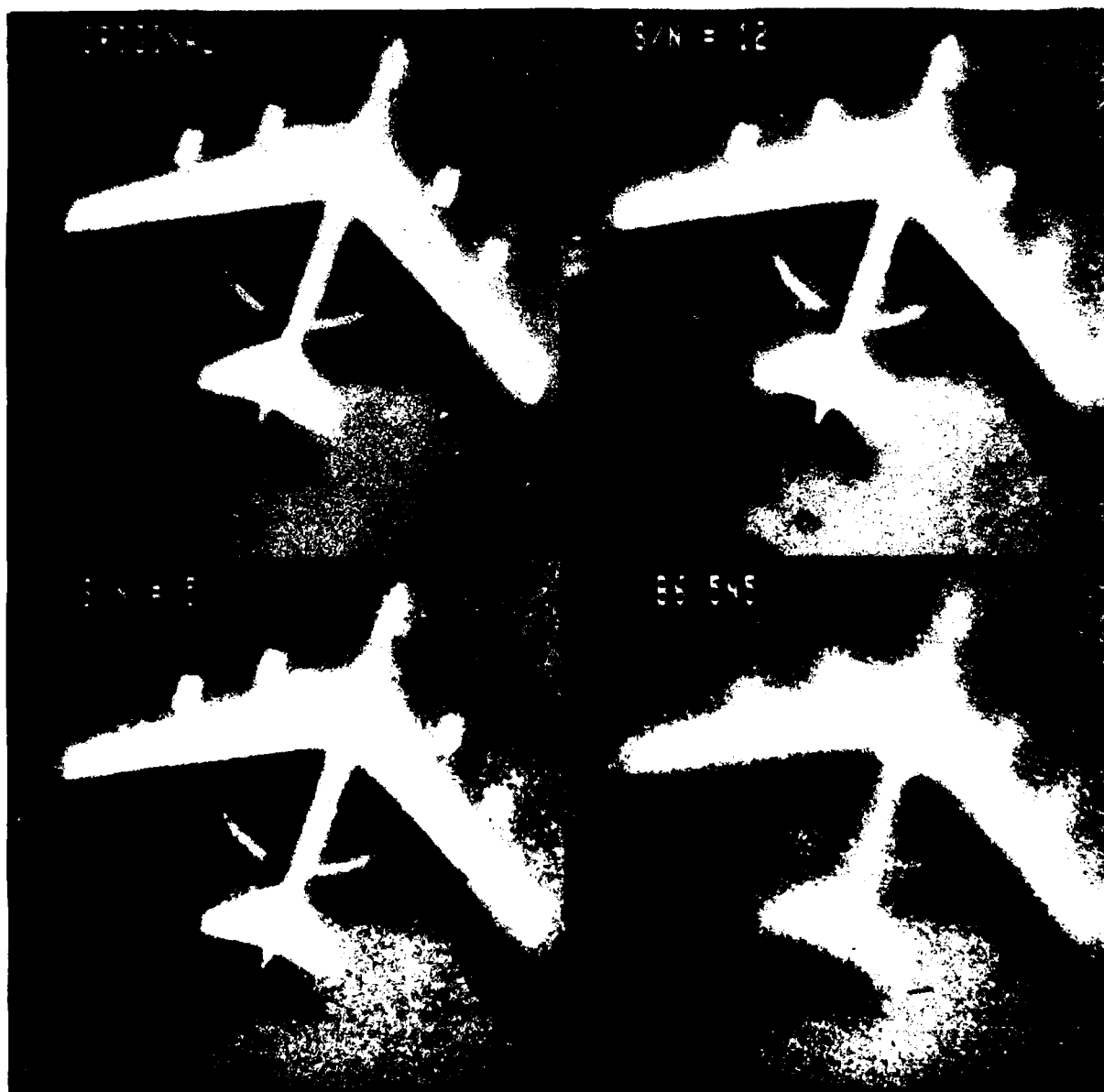


Figure 2 Original Image with Two Levels of Noise Degradation

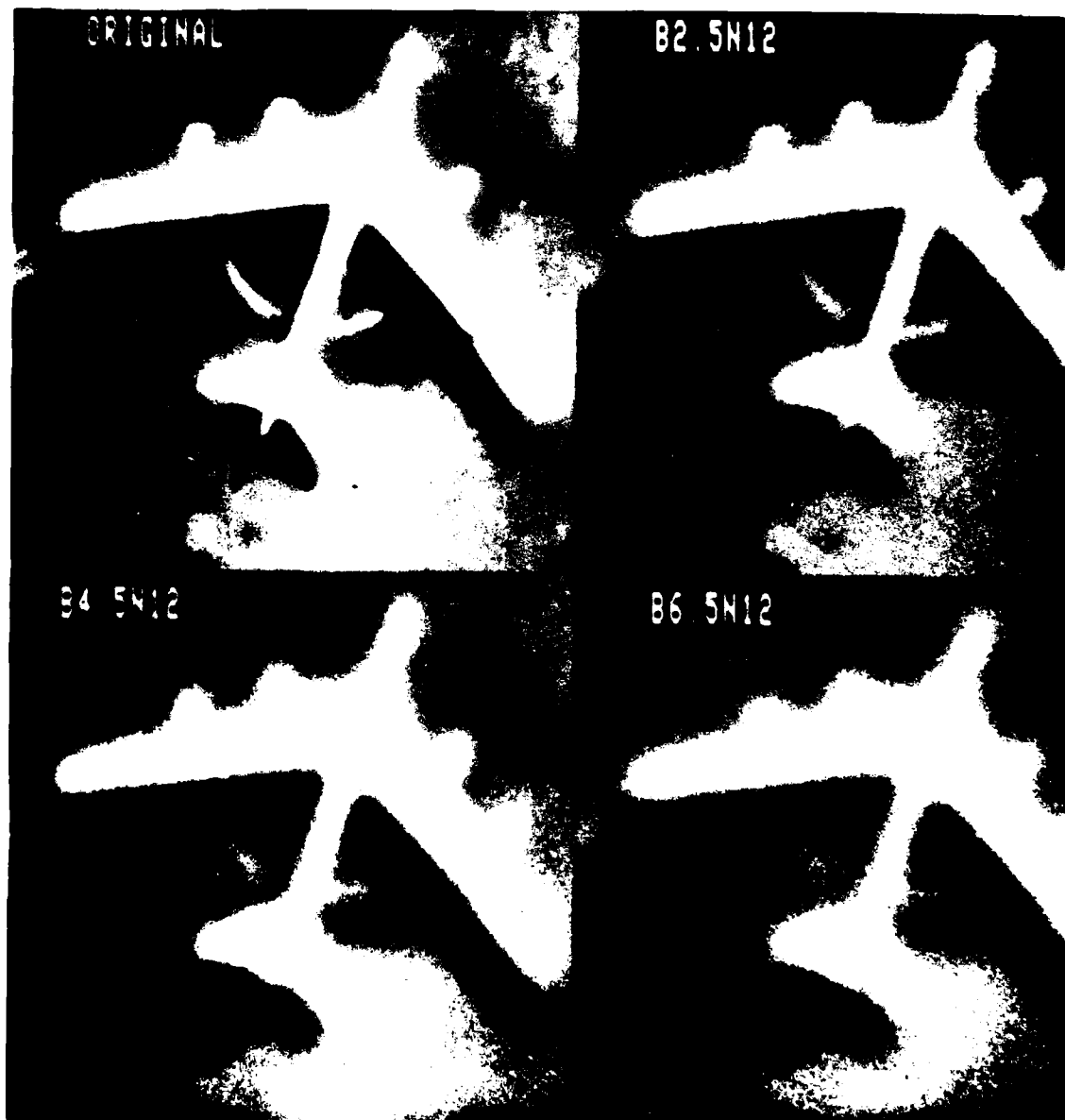


Figure 3 Original Image with Constant Noise Level and Various Blurs



Figure 4 Original Image Depicting Supervised Training Regions

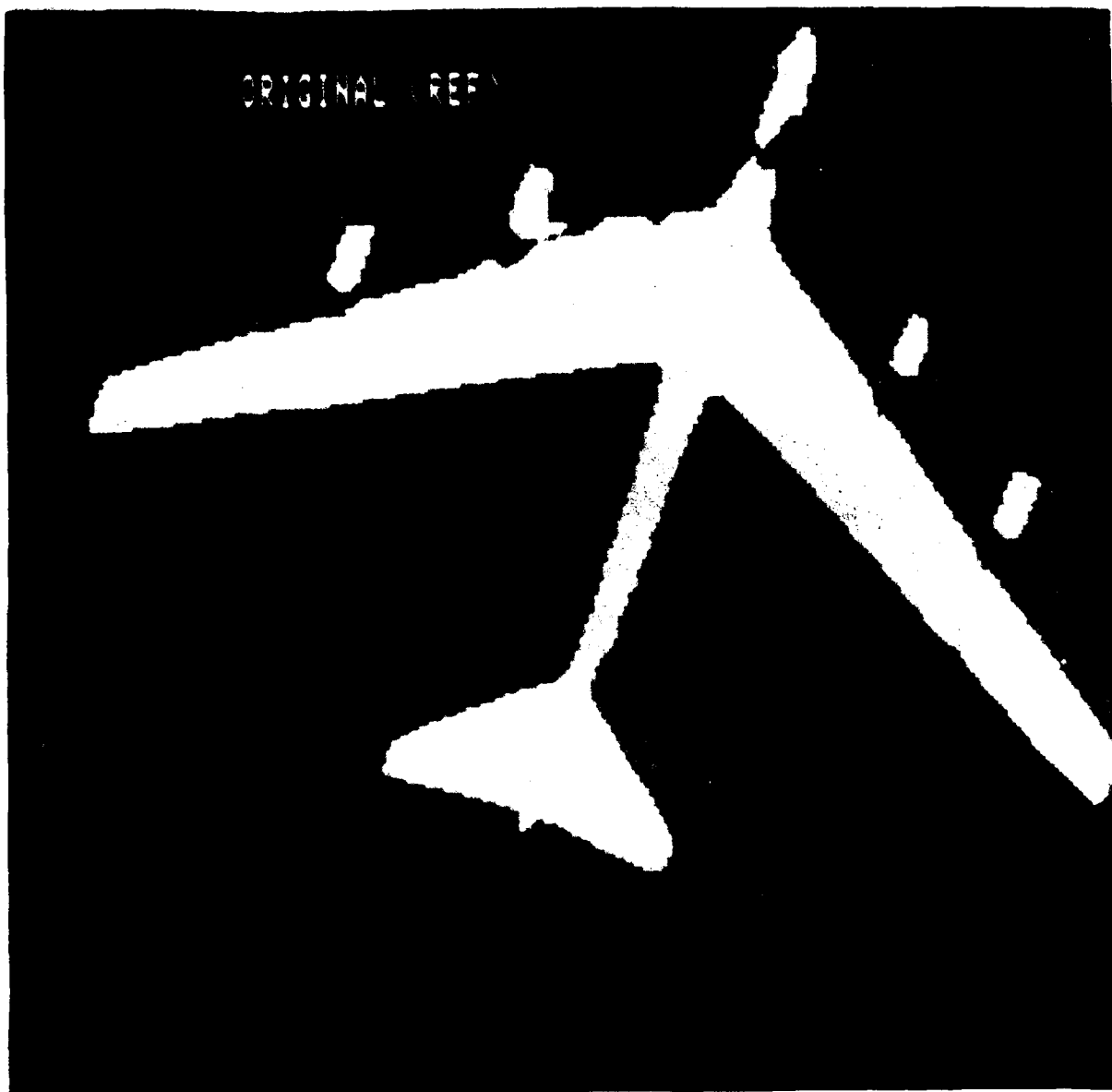


Figure 5 Original Images/Classification via AFES Software

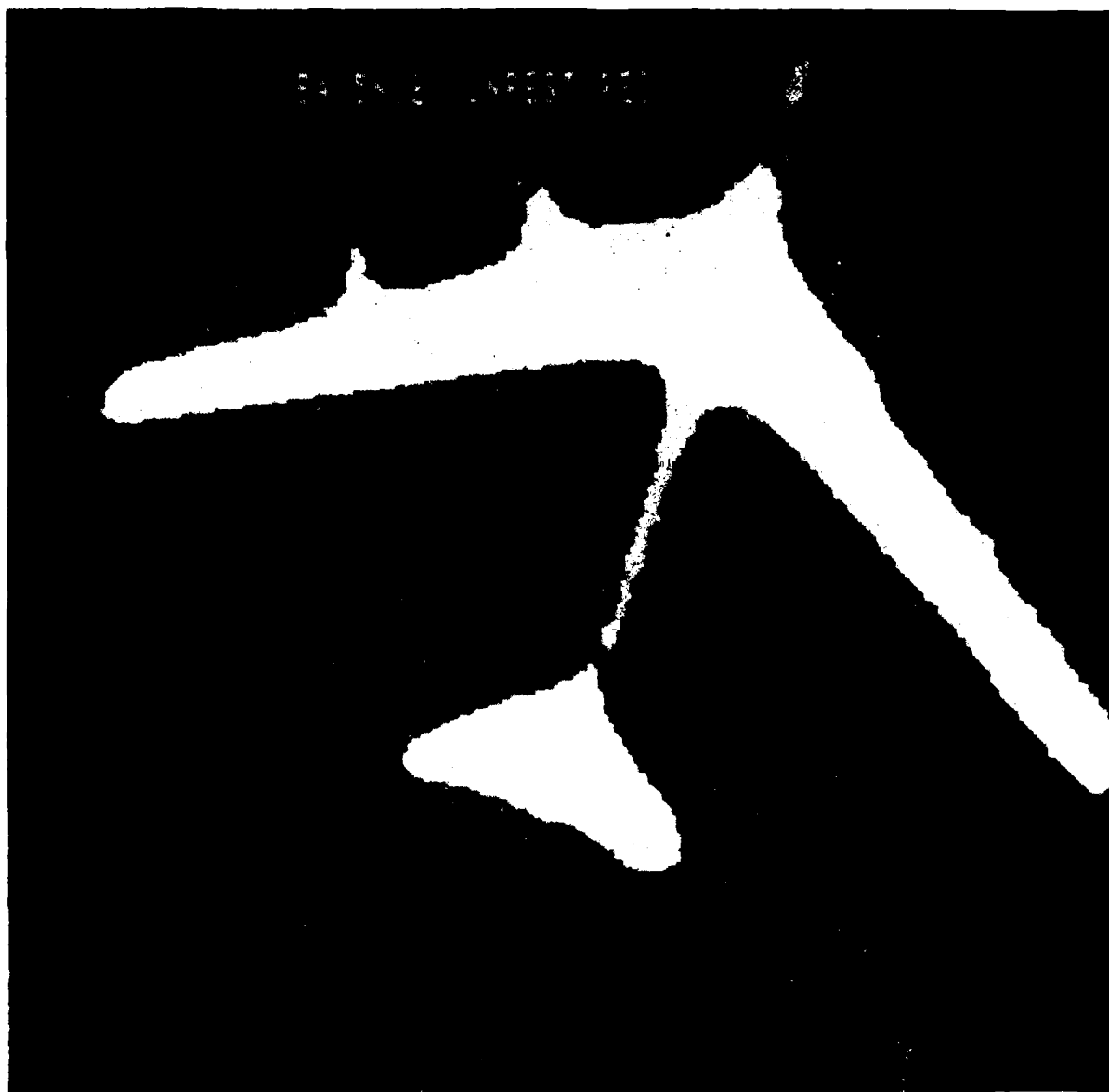


Figure 6 Classification Results on Degraded/Unrestored Image

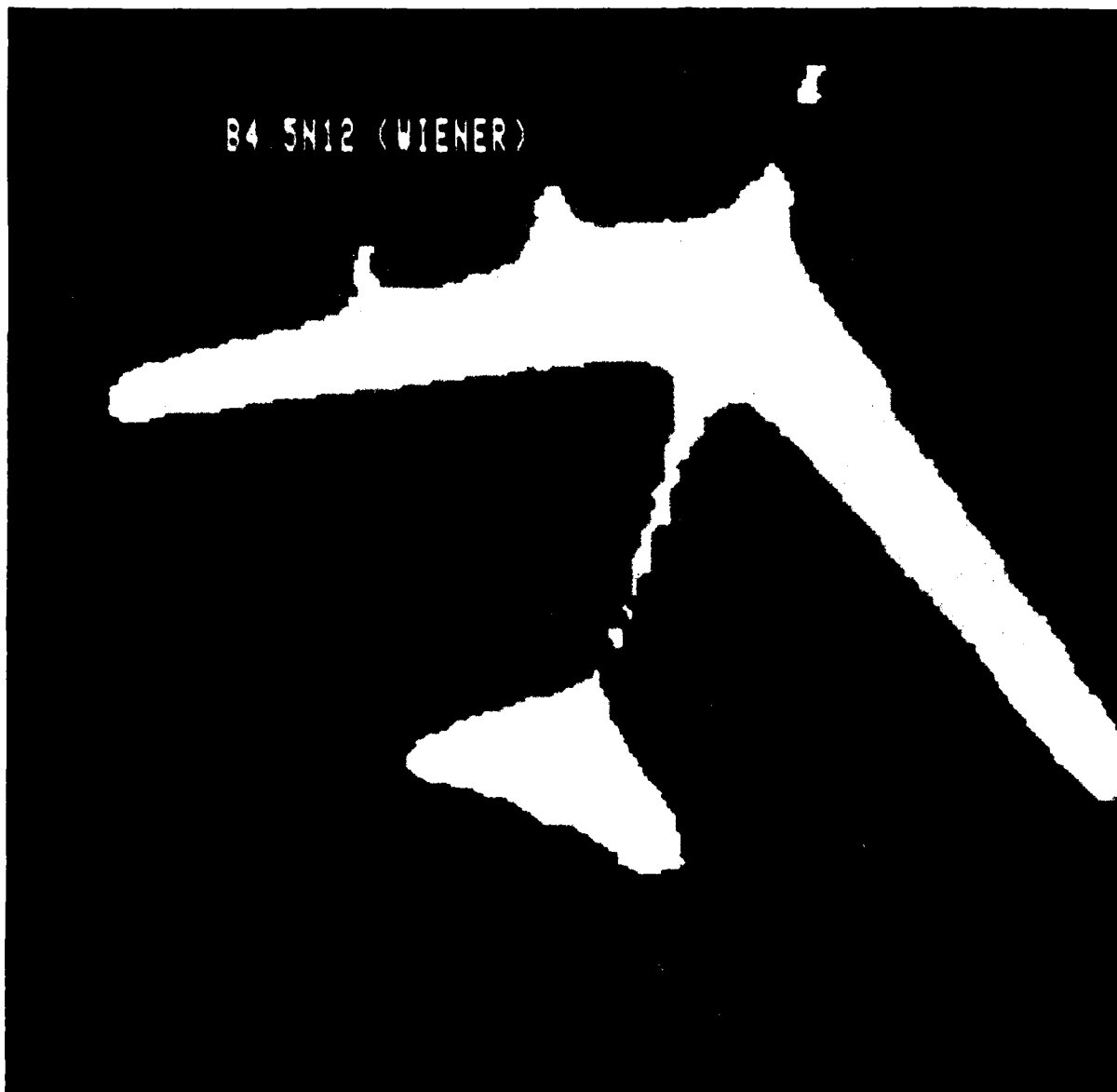


Figure 7 Classification Results on Degraded/Wiener Restored Image

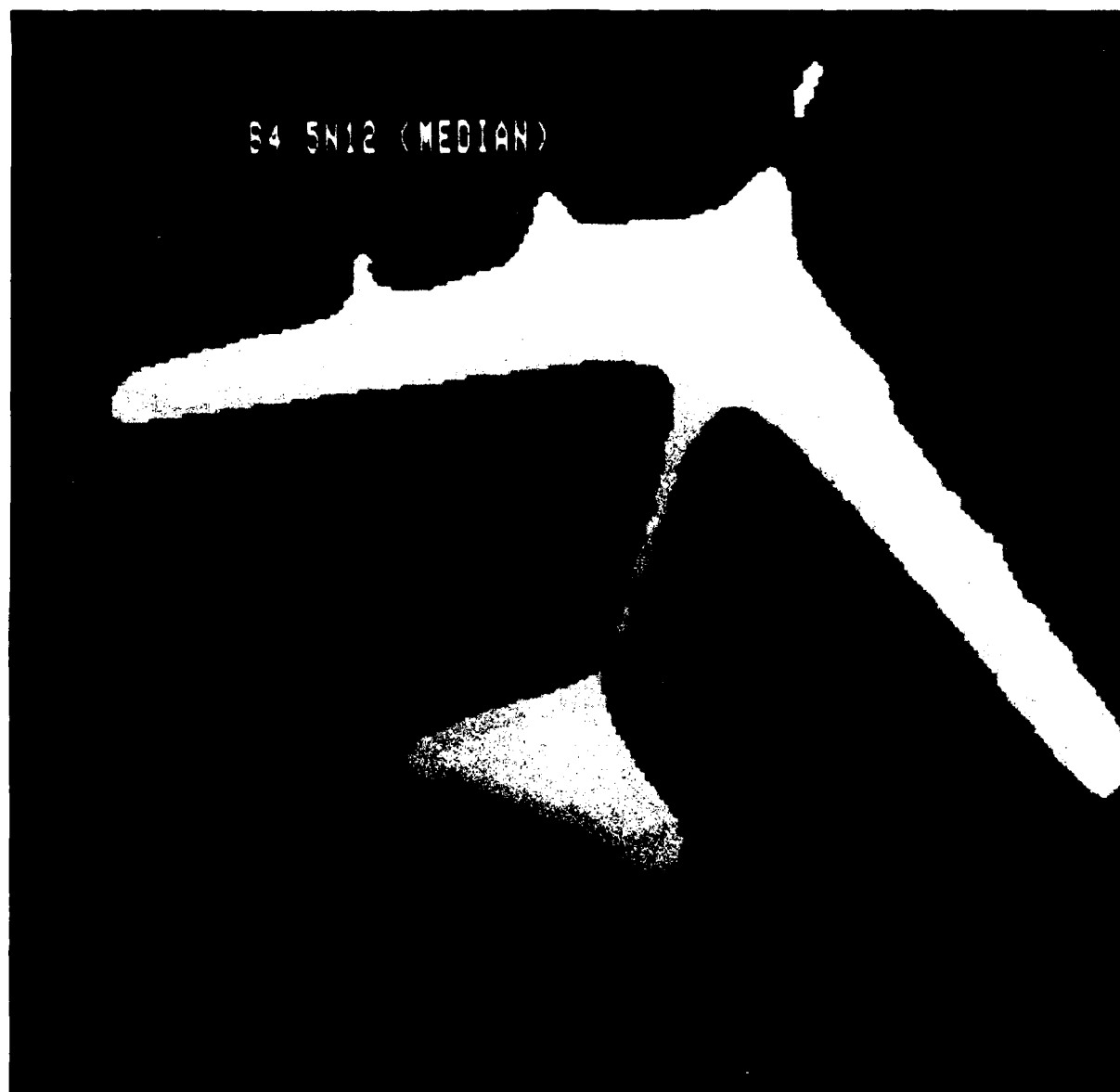


Figure 8 Classification Results on Degraded/Median Restored Image

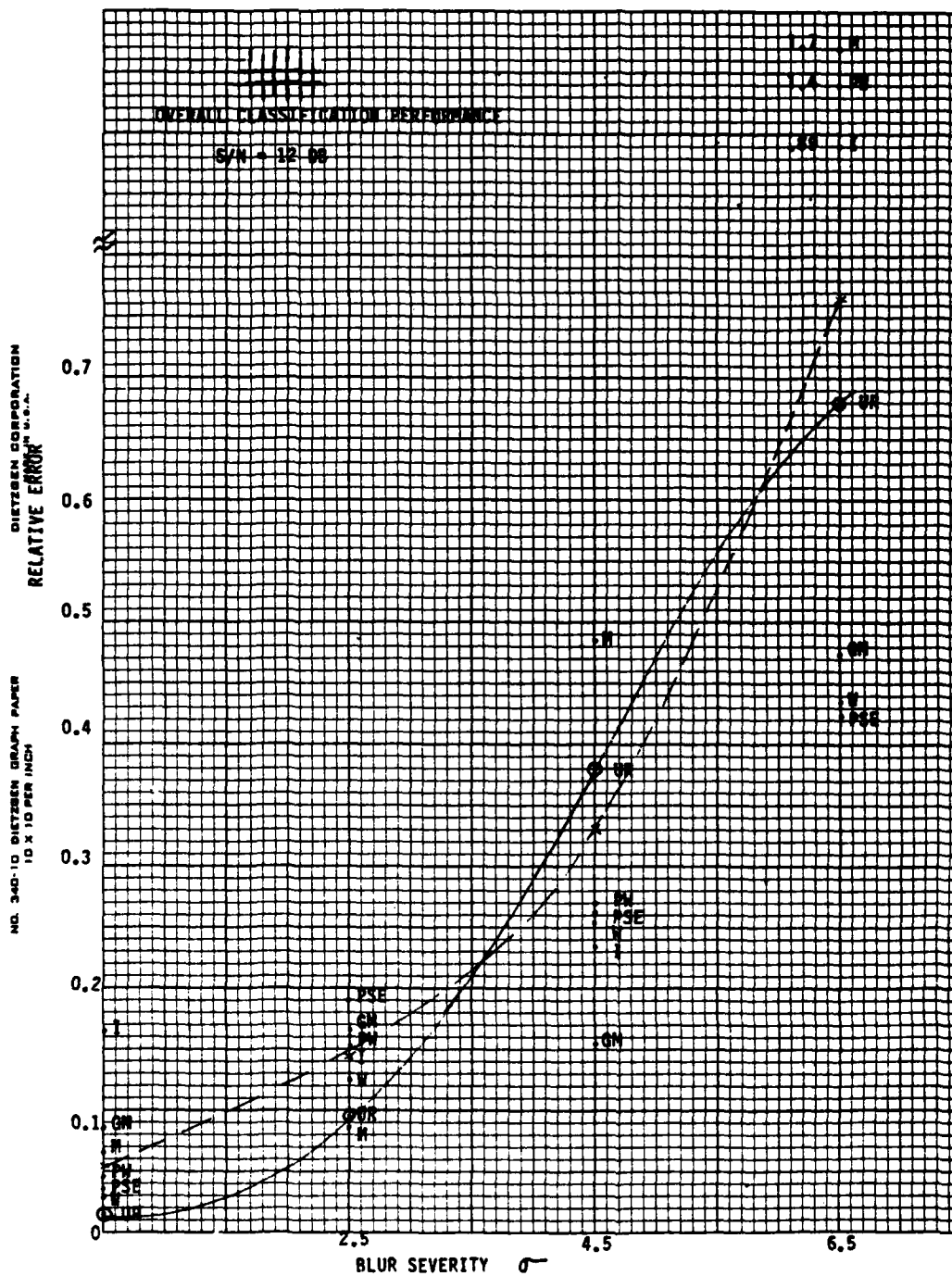


Figure 9 Overall Classification Performance



Figure 10 A Test Image Restored via Wiener,  
Median and Geometric Mean Filtering

## REFERENCES

1. H.C. Andrews and B. R. Hunt, Digital Image Restoration, (Prentice-Hall, Englewood Cliffs, N.J. 1977), pp. 113 - 208.
2. W. K. Pratt, Digital Image Processing, (J. Wiley, New York , 1978) pp. 378-446.
3. A. Rosenfeld and A.C. Kak, Digital Picture Processing, (Academic Press, New York, 1976), pp. 203 - 255.
4. R. C. Gonzalez and P. Wintz, Digital Image Processing, (Addison-Wesley, Reading, MA 1977), pp. 184 - 227.
5. E. L. Hall, Computer Image Processing and Recognition, (Academic Press, New York, 1979) pp. 214-247.
6. T. S. Huang (Ed), Picture Processing and Digital Filtering, 2nd Ed. (Springer-Verlag, New York, 1979), pp. 7-18, pp. 70-246, pp. 284-288.
7. T. S. Huang (Ed), Two-Dimensional Digital Signal Processing I., (Springer-Verlag, New York, 1981), pp. 4-7, pp. 11-40, pp. 155-205.
8. T. S. Huang (Ed), Two-Dimensional Digital Signal Processing II., (Springer-Verlag, New York 1981), pp. 161-217.
9. Op Cit Ref 1, pp. 159-160.
10. T.M. Cannon, H.J. Trussell, and B. R. Hunt, "Comparison of Image Restoration Methods," Applied Optics, Vol 17, No. 21, pp. 3384-3390, Nov 1978.
11. H. L. Snyder, M.E. Maddox, D.I. Shedivy, J.A. Turpin, J. J. Burke and R.N. Strickland, "Digital Image Quality and Interpretability: Database and Hardcopy Studies" Optical Engineering, Vol 21, No. 1, pp. 14-22, 1982.
12. G. Yang and T. S. Huang, "Median Filters and Their Applications to Image Processing", Tech Report., School of Electrical Engineering, Purdue Univ., 1980.
13. Op Cit Ref 4, pp. 215-217.
14. Op Cit Ref 1, pp. 160-161.
15. M. Cannon, "Blind Deconvolution of Spatially Invariant Image Blurs with Phase", IEEE Trans. ASSP24, No. 1, pp 58-63, Feb 1976.

16. J. W. Tukey, Exploratory Data Analysis, (Addison-Wesley, Reading, MA 1977).
17. T.S. Huang, G.J. Yang, G.Y. Tang., "A Fast Two-Dimensional Median Filtering Algorithm" IEEE Trans. ASSP-27, No. 1 pp. 13-18, Feb 1979.
18. E. Ataman, V.K. Aatre, K.M. Wong, "A Fast Method for Real-Time Median Filtering", IEEE Trans. ASSP-28, No. 4, pp 415-421, Aug 1980.
19. G. P. Wolfe, J.L. Mannos, "A Fast Median Filter Implementation", Proc. SPIE Seminar on Image Procesing, Sept 1979, San Deigo, CA
20. W.L. Evensole, D.J. Mayer, F.B. Frazee, T.F. Cheek, Jr., "Investigation of VLSI Technologies for Image Processing," Proc Image Understanding Workshop, Pittsburgh PA pp. 191-195, Nov 1978.
21. P.E. Hart, "The Condensed Nearest Neighbor Rule," IEEE Trsns. IT-14, No. 3. pp. 515-516, May 1968.
22. Op Cit Ref 1, pp. 124-125.



*MISSION  
of  
Rome Air Development Center*

*RADC plans and executes research, development, test and selected acquisition programs in support of Command, Control Communications and Intelligence (C<sup>3</sup>I) activities. Technical and engineering support within areas of technical competence is provided to ESD Program Offices (POs) and other ESD elements. The principal technical mission areas are communications, electromagnetic guidance and control, surveillance of ground and aerospace objects, intelligence data collection and handling, information system technology, ionospheric propagation, solid state sciences, microwave physics and electronic reliability, maintainability and compatibility.*

END

FILMED

9-84

DTIC





